A Genetic Algorithm for the Evaluation of Material Parameters of Compound Multilayered Structures

Thomas Zwick, *Member, IEEE*, Jens Haala, *Member, IEEE*, and Werner Wiesbeck, *Fellow, IEEE*

***Abstract*—This paper presents a new method to obtain the material parameters of each single layer in a multilayered structure. The compound structure has to be measured over frequency or for different incidence angles in the microwave frequency range. The genetic algorithm for parameter extraction from the reflection or transmission measurement data is based on a simplified evolution strategy. In this paper, the evolution optimization is described briefly and is verified by measurements performed in the frequency range from 115 to 145 GHz. The parameters obtained by the algorithm show good agreement with reference values gained by other researchers.**

***Index Terms*—Genetic algorithm, material parameter extraction, multilayered structure.**

I. Introduction

THE measurement of material properties is the basis for any theoretical design of electromagnetic devices. There are very accurate methods available for the determination of the permittivity and permeability of a given material [1]–[4]. However, these methods require a pure sample of the material that has to be measured. In this paper, a method is presented to measure material parameters of compound structures consisting of more than one layer. Typical examples are car windows or multilayered building walls. The permittivity and permeability of each single material is determined by a new genetic algorithm (GA) from measurements obtained over the frequency. The use of a GA makes this method very flexible, therefore, reflection measurements and/or transmission measurements may be used. If one has to determine highly dispersive materials, it is also possible to use this algorithm in combination with single frequency reflection or transmission measurements over different angles and for different polarizations. Another big advantage of the new method is that only scalar values without phases are required, which reduces the calibration effort drastically.

In this paper, the GA for this method is presented. For verification purposes, the results of two measurement campaigns have been used. The dielectric material parameters obtained by the new algorithm from angular-dependent measurements of the reflection coefficient of Quartz glass and Si_3N_4 at 140 GHz are compared to parameters obtained for the same materials with an open resonator method. To show its applicability on multilayered media, three plates consisting of Teflon, Macor, and Al_2O_3 have been measured in the frequency range from 115 to 145 GHz. The single plates have been measured as well as their different combinations. Additionally, these results are compared with values from the literature.

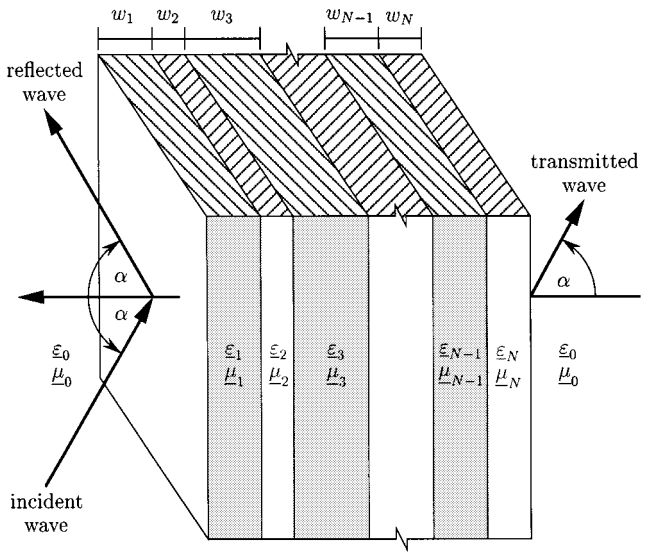

Fig. 1. Reflection and transmission of electromagnetic waves at multilayered structures.

II. Basic Theory

The reflection and transmission coefficients $\underline{R}$ and $\underline{T}$ of multilayered structures (see Fig. 1) can be analytically described as a function of permittivities $\underline{\varepsilon}_n$, permeabilities $\underline{\mu}_n$, and thicknesses ω_n of the N layers ($n = 1, \ldots, N$), the frequency f, and the incidence angle α

$$\underline{R}, \underline{T} = \mathrm{func}\Big(\alpha, f, \underline{\varepsilon}_1, \underline{\mu}_1, w_1, \underline{\varepsilon}_2, \underline{\mu}_2, w_2, \ldots, \underline{\varepsilon}_N, \underline{\mu}_N, w_N\Big). \tag{1}$$

If all parameters are known, the reflection or transmission coefficients can be calculated by a fast recursive method, as described in [5]. Thereby each layer has to be plane, smooth, and infinite.

If one wants to obtain the material parameters from the reflection or transmission coefficients, the problem becomes an under-determined system of nonlinear equations. Therefore, it is not possible to determine permittivity and permeability of a multilayered structure from a single measurement of reflection

Manuscript received October 4, 2000; revised April 24, 2001.

T. Zwick was with the Institut für Höchstfrequenztechnik und Elektronik, Universität Karlsruhe, 76128 Karlsruhe, Germany. He is now with the IBM T. J. Watson Research Center, Yorktown Heights, NY 10598 USA (e-mail: zwick1@us.ibm.com).

J. Haala was with the Institut für Höchstfrequenztechnik und Elektronik, Universität Karlsruhe, 76128 Karlsruhe, Germany. He is now with Marconi Communications Software Systems, 71509 Backnang, Germany (e-mail: Jens.Haala@marconi.com).

W. Wiesbeck is with the Institut für Höchstfrequenztechnik und Elektronik, Universität Karlsruhe, 76128 Karlsruhe, Germany (e-mail: Werner.Wiesbeck@etec.uni-karlsruhe.de).

Publisher Item Identifier S 0018-9480(02)03034-X.

0018-9480/02$17.00 © 2002 IEEE

and/or transmission. To gather enough information for solving this problem, one has to perform additional measurements. These may be measurements over a certain frequency range or otherwise over different angles of incidence.

It is further not possible to invert the system of equations to solve for the material parameters if more than one layer is present. Therefore, a new procedure was developed that allows to calculate the material parameters of multilayered structures by means of stepwise optimization. This optimization problem exhibits many local optima making traditional optimization algorithms, such as the gradient method, unfavorable. A new procedure has been developed based on the method of evolution optimization, as published by Rechenberg and Goldberg [6], [7]. The material parameters of the individual layers of a compound structure are found by minimizing the error between values obtained from (1) and measurements. An overview about GAs in electrical engineering can be found in [8] and [9].

III. Evolution Strategy

In this section, the evolution strategy adapted to the given problem is described in detail (the vector notation is used in an incorrect form to simplify the formulations: *all vector operations are meant element-wise*).

The idea of evolution optimization is based on the biological process of the natural selection in evolution. Transferred to the problem discussed here, generations of data sets $\vec{\lambda}$ are produced randomly where each generation is deduced from the "best" data set of the previous generation (natural selection/only the fittest survive). This data set is called "parent." In contrast to the natural evolution here, only one parent is used and all offsprings are generated by "mutation." An appropriate evolution optimization method has been developed for the special peculiarities of the present problem. The total cycle of the method is illustrated as a flowchart in Fig. 2.

All unknowns $\lambda^1, \lambda^2, \ldots, \lambda^L$ (L: total number of unknowns) that have to be determined are stored in the parameter vector

$$\vec{\lambda} = \left(\lambda^1, \lambda^2, \ldots, \lambda^L\right)^T. \tag{2}$$

The unknowns are the real and imaginary parts of the complex material parameters $\underline{\varepsilon}_n$, $\underline{\mu}_n$ and the thicknesses w_n of the arbitrary, but known number of layers N. Simulations performed with the measurements of Section IV showed that the determination of the thicknesses of the layers together with their dielectric parameters results in a much larger error. Therefore, and because of the fact that mostly the thicknesses can be more accurately measured by physical means, the determination of thicknesses is not investigated in this paper even though it is principally possible with the GA.

The population size of each generation is given by M. Based on the parent data vector $\vec{\lambda}_{g,\mathrm{parent}}$, the M data sets $\vec{\lambda}_{g,m}$ ($m = 1, \ldots, M$) of the gth generation are randomly generated according to

$$\vec{\lambda}_{g,m} = \vec{\lambda}_{g,\mathrm{parent}} \cdot e^{\mathcal{N}\left(\vec{0},\vec{\sigma}_g\right)}. \tag{3}$$

As already noted in (3), each element of the vector $\vec{\lambda}_{g,m}$ is generated by multiplication of $\vec{\lambda}_{g,\mathrm{parent}}$ with the exponential of a normal distributed random variable with zero mean. The standard deviation is the corresponding component of the vector $\vec{\sigma}_g$. For each element ℓ with $\ell = 1, \ldots, L$ of $\vec{\lambda}_{g,m}$ (3) can be rewritten as

$$\lambda^{\ell}_{g,m} = \lambda^{\ell}_{g,\mathrm{parent}} \cdot e^{\mathcal{N}\left(0,\sigma^{\ell}_g\right)}. \tag{4}$$

The use of the normal distribution causes the algorithm to mainly search in the near range of $\lambda_{g,\mathrm{parent}}$ where the solution is expected to be. Additionally, the unknowns $\vec{\lambda}_{g,m}$ have a lower and upper limit $\vec{\lambda}_{\min}$ and $\vec{\lambda}_{\max}$, respectively. These limits can be taken from the literature [5], [10] or chosen from the best available knowledge.

The measured reflection or transmission coefficients in decibels are defined by A_k ($k = 1, \ldots, K$) over K frequency points or angles of incidence, respectively, depending on which of both have been varied during the measurement. As demonstrated in Section IV, the use of the values in decibels instead of linear values leads to a very much better performance of the algorithm because the characteristic minima of the curves are better taken into account. $A'_{k,g,m}$ represents the simulated reflection or transmission coefficients curve using the current data set $\vec{\lambda}_{g,m}$. The error criterion to qualitatively evaluate the data set $\vec{\lambda}_{g,m}$ is the normalized root mean square (rms)

$$\Delta_{g,m} = \sqrt{\frac{1}{K}\sum_{k=1}^{K}\left(A_k - A'_{k,g,m}\right)^2} \tag{5}$$

where $\Delta_{g,m}$ is called the "fitness function." In order to avoid effects caused by the limited dynamic range of the measurement system, all values (measured and simulated) are limited to the sensitivity level of the measurement system. If more than one curve (e.g., over the frequency and over the angle) is available, the total information can be used by just adding the fitness functions (5) of all curves. The phase information is not taken into account, which is the big advantage of this method because, especially at millimeter-wave frequencies, scalar measurements are much easier.

By applying the fitness function (5), the best data vector $\vec{\lambda}_{g,\mathrm{best}}$ of the gth generation can be found as the vector $\vec{\lambda}_{g,m}(m = 1, \ldots, M)$, which belongs to the smallest $\Delta_{g,m}$. It is additionally tested if the best data vector of the previous generation $\vec{\lambda}_{g-1,\mathrm{best}}$ has a smaller error.

As parent vector $\vec{\lambda}_{\mathrm{parent},g}$ for the gth generation, the best parameter vector found in the previous generation is used

$$\vec{\lambda}_{g,\mathrm{parent}} = \vec{\lambda}_{g-1,\mathrm{best}}. \tag{6}$$

The first generation is set using approximate values

$$\vec{\lambda}_{1,\mathrm{parent}} = \vec{\lambda}_{\mathrm{start}} \tag{7}$$

taken from the literature [5], [10] or chosen from the best available knowledge. All simulations showed that the choice of the initial values has no effect on the total performance.

Each time a new generation is developed, the standard deviation is reduced by

$$\vec{\sigma}_g = v_\sigma \cdot \vec{\sigma}_{g-1}, \qquad \text{with } 0 < v_\sigma < 1 \tag{8}$$

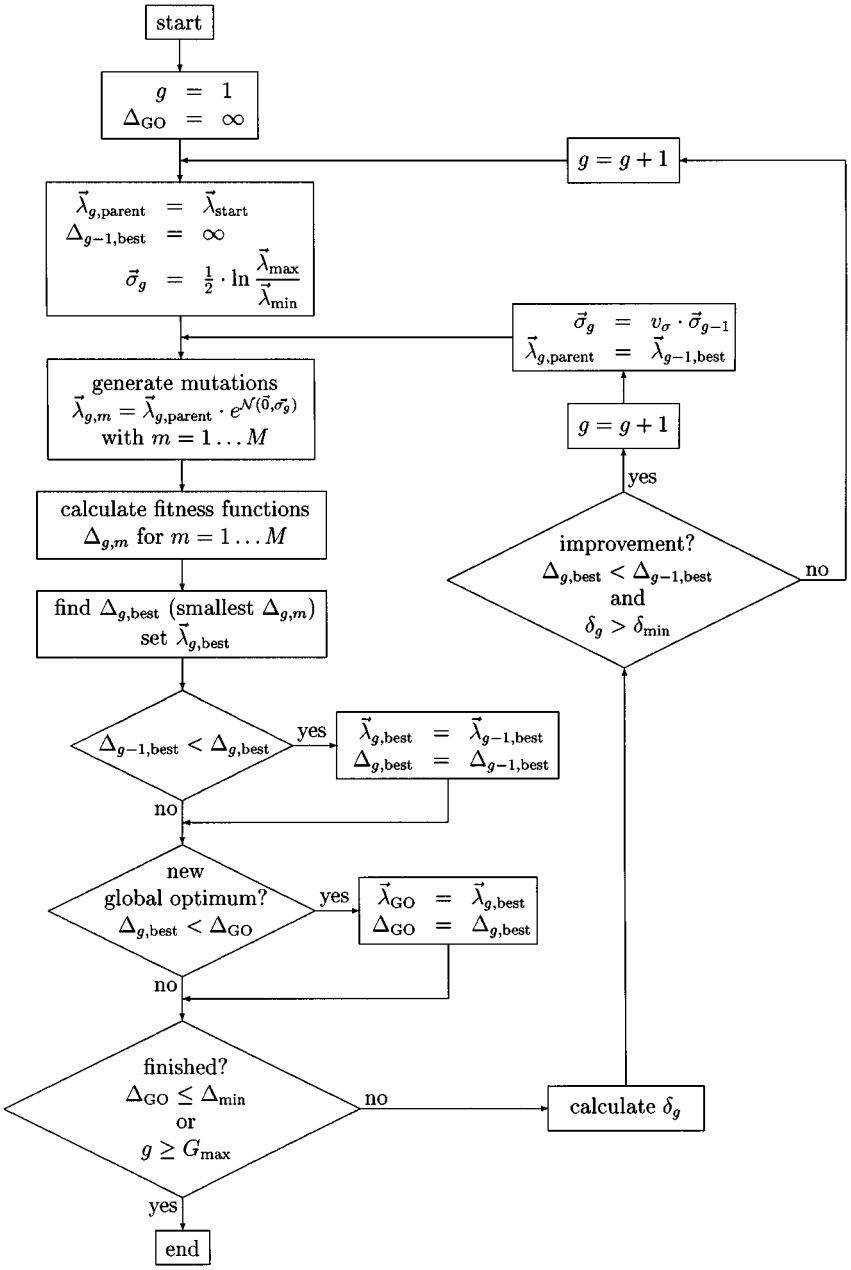

Fig. 2. Evolution strategy.

in order to reduce the search space as the GA comes closer to a solution. $v_\sigma = 0.5$ has been found to provide the best performance. As initial value

$$\vec{\sigma}_1 = \frac{1}{2} \ln \frac{\vec{\lambda}_{\max}}{\vec{\lambda}_{\min}} \tag{9}$$

is reasonable, which again, is meant element-wise as follows:

$$\sigma_1^\ell = \frac{1}{2} \ln \frac{\lambda_{\max}^\ell}{\lambda_{\min}^\ell}. \tag{10}$$

This iterative process of producing generations of data sets $\vec{\lambda}_{g,m}$ is continued until no further reduction of the error $\Delta_{\mathrm{best},g}$ compared to the minimal error of the previous generation $\Delta_{\mathrm{best},g-1}$ is reached or the relative error variation

$$\delta_g = \frac{\sigma_{\Delta,g}}{\mu_{\Delta,g}} \tag{11}$$

with

$$\mu_{\Delta,g} = \frac{1}{M} \sum_{m=1}^{M} \Delta_{g,m} \tag{12}$$

and

$$\sigma_{\Delta,g} = \sqrt{\frac{1}{M} \sum_{m=1}^{M} \left(\Delta_{g,m} - \mu_{\Delta,g} \right)} \tag{13}$$

falls below a given limit of $\delta_{\min}$. This avoids losing computing time by creeping convergence.

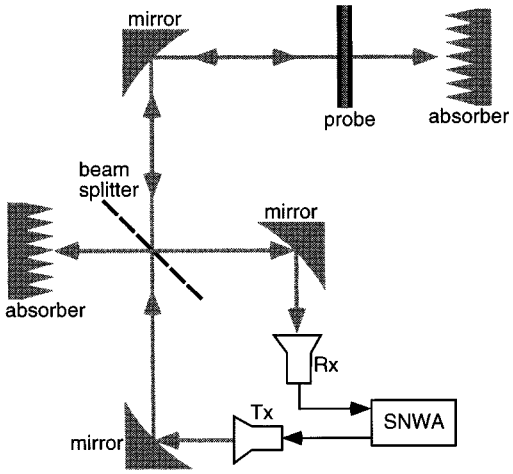

Fig. 3. Quasi-optical millimeter-wave reflection measurement setup for perpendicular incidence.

In order to increase the probability that the global optimum (GO) is found, the whole process described above has to be started again several times. Thereby several local optima and very probably the GO given by $\vec{\lambda}_{\mathrm{GO}}$ and the dedicated fitness function Δ_{GO} will be found (see Fig. 2). The relatively large initial values for the standard deviation (9) guarantee that different local optima are found in spite of always using the same initial values for λ (7). The evolution optimization process is finished if a minimum error $\Delta_{\min}$ or a total number of generations $G_{\max}$ is reached.

IV. Measurement and Simulation Results

Two measurement campaigns were performed to validate the performance of the new method. The measurement system is based on a scalar network analyzer (SNWA) with a frequency accuracy of 1 MHz. The setup is sketched in Fig. 3 and described in detail in [11] and [12]. Wide-band corrugated horn antennas as transmitter (Tx) and receiver (Rx) together with focusing metallic ellipsoidal mirrors generates a Gaussian beam ($\mathrm{TEM}_{0,0}$). The waist radius of the beam at the probe is less than 25 mm in the frequency range from 115 to 145 GHz. This yields an angular incidence variation of the beam at the probe below 2.5°. Therefore, the beam is assumed to be a plane wave. In order to measure the reflection coefficient for perpendicular incidence, a thin polyester foil (Mylar) is used as beam splitter. The quasi-optical measurement setup, as shown in Fig. 3, enables the measurement of the scalar reflection loss versus frequency for perpendicular incidence. For calibration, the probe is replaced by a metal plate. With an extra mirror for the separation of the reflected beam from the transmitted beam, angular-dependent measurements are possible. Thereby a stepping motor controls the angle of the probe and the reflected beam including the Rx antenna in order to ensure precise specular reflection. This extension allows the determination of the scalar reflection loss from 10° to 80° of incidence. The setup for angle dependent measurements is described in detail in [14].

TABLE I
Start Vector $\vec{\lambda}_{\mathrm{start}}$ and Limitation Values $\vec{\lambda}_{\min}$ and $\vec{\lambda}_{\max}$ Used for the Simulations

	Quartz-glass		Si_3N_4		Al_2O_3		Macor		Teflon	
	ε'	$\tan\delta$	ε'	$\tan\delta$	ε'	$\tan\delta$	ε'	$\tan\delta$	ε'	$\tan\delta$
$\vec{\lambda}_{\mathrm{start}}$	5	0.01	5	0.01	5	0.01	5	0.01	5	0.01
$\vec{\lambda}_{\min}$	1	10^{-5}	1	10^{-5}	1	10^{-5}	1	10^{-5}	1	10^{-5}
$\vec{\lambda}_{\max}$	10	0.1	10	0.1	20	0.1	10	0.1	10	0.1

A. Measurements of Single Layers

In the following, the results of two different measurement campaigns are used to investigate the performance of the new method for single-layered media in comparison with results from literature.

1) Angular-Dependent Measurements of Single Layers: The reflection losses of two different plates of Quartz glass and Si_3N_4 have been measured over the incidence angles from 10° to 80° at a frequency of 140 GHz for both perpendicular (TE) and parallel (TM) polarization [13]. The size of the rectangular plate of Quartz glass is 215 mm × 95 mm with a thickness of 7.04 mm. The Si_3N_4 plate has a size of 320 mm × 120 mm and a thickness of 3.163 mm. The parameter vector (2) for these one-layered materials with known thicknesses reduces to

$$\vec{\lambda} = \left(\varepsilon', \tan\delta\right)^T \tag{14}$$

with $\underline{\varepsilon} = \varepsilon_0(\varepsilon' - j\varepsilon'\tan\delta)$. The permeability can be assumed to be $\underline{\mu} = \mu_0$. For all simulations with respect to the angular-dependent measurements $G_{\max} = 500$, $v_\sigma = 0.5$, $M = 500$, and a sensitivity level of −30 dB is used. The limits and starting values for the simulations are given in Table I. The material parameters of these three materials were already measured with an open resonator method by [1].

In Figs. 4 and 5, the measured and simulated (from the values obtained by the GA) reflection losses over the incidence angle α are plotted for both polarizations. The very good match of the curves demonstrates the validity of the method. In Table II, the results of the measurements in combination with the new algorithm are compared to the values obtained from literature. A very good agreement for the real part of the permittivity of both materials is observed. The imaginary parts cannot be determined with the same accuracy. This inaccuracy is caused by the limited sensitivity level of the measurement system because the imaginary part is determined by the depth of the minimum. Additionally, two different kinds of characteristic minima can be observed in Figs. 4 and 5. The first minimum is caused by negative interference of multiple reflections inside the plate and is, therefore, observed at both polarizations. The second minimum arises at the Brewster angle. Both characteristic minima are important for the performance of the method and define the necessary angular range.

2) Frequency-Dependent Measurements of Single Layers at Perpendicular Incidence: The scalar reflection losses of three circular plates of the materials: 1) Al_2O_3: poly-crystalline Al_2O_3 with 97.6% purity; 2) Macor: Corning Macor Machinable Glass Ceramic is a product of Corning Glass Works,

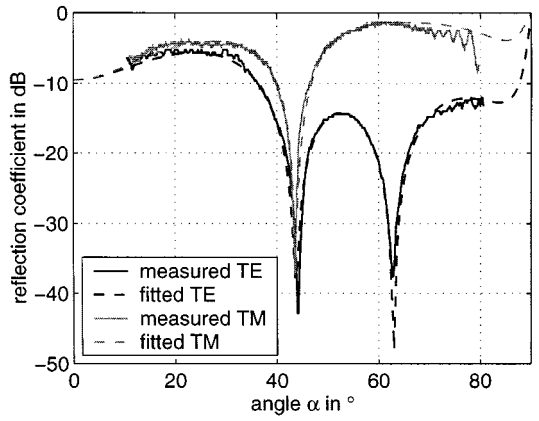

Fig. 4. Reflection coefficient over the incidence angle α at Quartz glass for perpendicular (TE) and parallel (TM) polarization at 140 GHz.

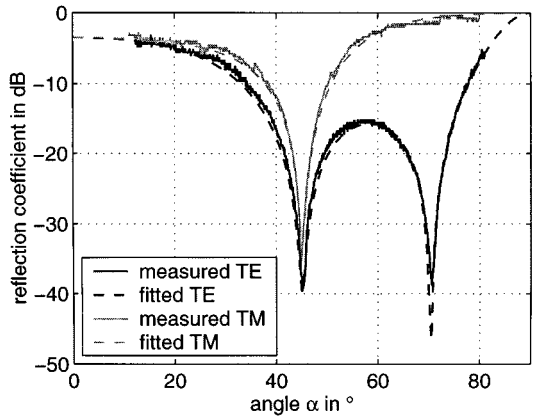

Fig. 5. Reflection coefficient over the incidence angle α at Si_3N_4 for perpendicular (TE) and parallel (TM) polarization at 140 GHz.

TABLE II
COMPARISON OF THE MATERIAL PARAMETERS OF QUARTZ GLASS AND Si_3N_4 OBTAINED FROM THE ANGULAR DEPENDENT MEASUREMENTS WITH THE REFERENCE VALUES

	Quartz-glass		Si_3N_4	
	ε'	$\tan\delta$	ε'	$\tan\delta$
literature [1]	3.80	$0.45 \cdot 10^{-3}$	7.83	$0.34 \cdot 10^{-3}$
single layers	3.81	$1.10 \cdot 10^{-3}$	7.84	$1.00 \cdot 10^{-3}$

Corning, NY; and 3) Teflon have been measured in the frequency range from 115 to 145 GHz at perpendicular incidence. The diameter of all plates is 70 mm. Their thicknesses are physically measured with an accuracy of 10 μm to 3.407 mm (Al_2O_3), 3.15 mm (Macor), and 5.63 mm (Teflon). For the measurements

$$\vec{\lambda} = (\varepsilon', \tan\delta)^T \tag{15}$$

with $\underline{\varepsilon} = \varepsilon_0(\varepsilon' - j\varepsilon'\tan\delta)$ and $\underline{\mu} = \mu_0$ is used. All simulations are performed with the parameters $G_{\max} = 2000$, $v_\sigma = 0.5$, and $M = 500$, and a sensitivity level of -15 dB is used. The limits and starting values for the simulations are given in Table I. The material parameters of these three materials were already measured in the frequency range of interest with other methods

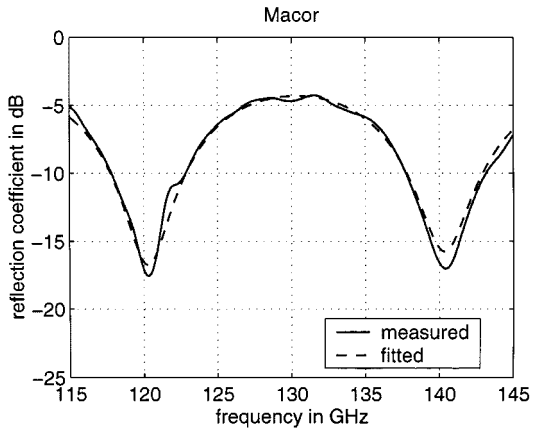

Fig. 6. Reflection coefficient versus frequency for Macor at perpendicular incidence.

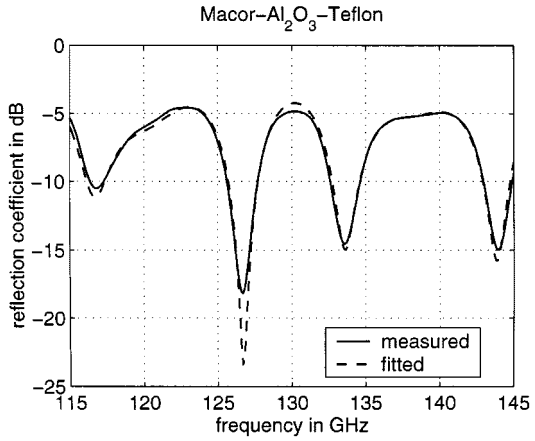

Fig. 7. Reflection coefficient versus frequency for Macor–Al_2O_3–Teflon at perpendicular incidence.

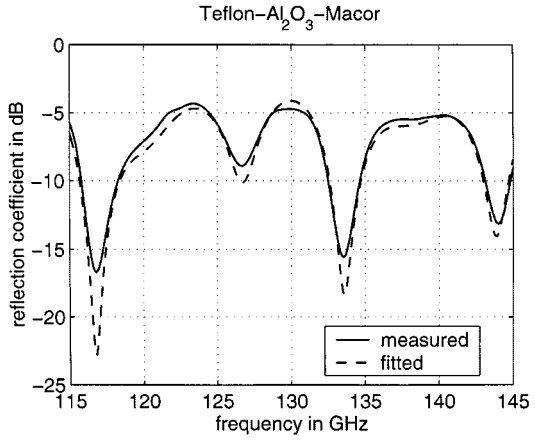

Fig. 8. Reflection coefficient versus frequency for Teflon–Al_2O_3–Macor at perpendicular incidence.

[2]–[4]. The values for Al_2O_3 could only be used as clue because, in [2], a probe with slightly different consistence was used.

In Fig. 6, the reflection coefficient of Macor is given versus frequency together with the corresponding simulations. One can see that the simulated curve fits very well to the measured curve. Similar results have been obtained for the other two materials.

TABLE III
COMPARISON OF THE MATERIAL PARAMETERS OF Al_2O_3, MACOR, AND TEFLON OBTAINED FROM MEASURING ALL COMBINATIONS OVER THE FREQUENCY COMPARED TO THE REFERENCE VALUES

measured	Al_2O_3		Macor		Teflon	
structures	ε'	$\tan\delta$	ε'	$\tan\delta$	ε'	$\tan\delta$
literature [2, 3, 4]	$9.5-10.1$	$0.2-0.8\cdot10^{-3}$	5.66	0.017	2.05	$3\cdot10^{-3}$
single layers	9.21	$3.12\cdot10^{-3}$	5.63	0.020	2.05	$2.12\cdot10^{-3}$
Al_2O_3-Macor	9.10	$0.01\cdot10^{-3}$	5.78	0.023	-	-
Al_2O_3-Teflon	9.20	$2.63\cdot10^{-3}$	-	-	2.08	$0.01\cdot10^{-3}$
Macor-Teflon	-	-	5.61	0.016	2.05	$0.01\cdot10^{-3}$
Al_2O_3-Macor-Teflon	9.07	$0.08\cdot10^{-3}$	5.75	0.018	2.09	$0.01\cdot10^{-3}$
Al_2O_3-Teflon-Macor	9.19	$0.60\cdot10^{-3}$	5.60	0.008	2.09	$10.10\cdot10^{-3}$
Macor-Al_2O_3-Teflon	9.05	$0.02\cdot10^{-3}$	5.78	0.020	2.09	$0.04\cdot10^{-3}$

Again, characteristic minima caused by negative interference are observed, which are important for the performance of the method. The measurements have to be performed over sufficient bandwidth to produce these characteristic minima. The good match of the fitted curve with the measured curve in Fig. 6 also proves that the materials are not highly dispersive and, therefore, have nearly constant parameters in the frequency range of interest. This can also be seen in [3] where the parameters for Macor are frequency independent in the range from 115 to 145 GHz.

B. Measurements of Compound Multilayered Structures

As already mentioned, the main advantage of the new method is the possibility of measuring compound multilayered structures and extracting the material parameters of all layers. The validity of the new method for multilayered media is shown for the three circular plates from Section IV-A.2, measured in different combinations. For the measurements, $\underline{\varepsilon}_n = \varepsilon_0(\varepsilon'_n - j\varepsilon'_n\tan\delta_n)$ and $\underline{\mu}_n = \mu_0$ can be used. The parameter vector (2) is then given by

$$\vec{\lambda} = \left(\varepsilon'_1, \tan\delta_1, \varepsilon'_2, \tan\delta_2, \ldots, \varepsilon'_N, \tan\delta_N\right)^T \tag{16}$$

with $L = 2N$. The measurements of the compound structures can be divided into the following two groups: 1) two materials at a time are combined and measured from each side ($N = 2$) and 2) all three materials are combined in different orders and measured from each side ($N = 3$). The measurements are performed from both sides of the multilayered structure and both curves are used for the parameter evaluation. Again, all simulations are performed with the parameters $G_{\max} = 2000$, $v_\sigma = 0.5$, and $M = 500$, and a sensitivity level of -15 dB is used. The limits and starting values for the simulations are given in Table I.

In Figs. 7 and 8, the reflection coefficients of Macor–Al_2O_3–Teflon, measured from both sides of the structure, are given versus frequency together with the corresponding simulations. In both cases, one can see that the simulated curves fit very well to the measured curves of the multilayered structures. Similar results have been obtained for all other combinations of the three materials. Again, characteristic minima caused by negative interference are observed, which are important for the performance of the method. The good match of the curves in Figs. 7 and 8 proves the frequency independence of the materials.

The material parameters determined from the measurements together with the new algorithm are given in Table III. It can be seen that there is only a small loss in accuracy when measuring the multilayered structure instead of separately measuring the three layers. The imaginary parts of the permittivities cannot be accurately determined, except for Macor. In contrast, the real permittivities ε' of all three materials can be very accurately determined (see Table III). The root mean square relative error of ε' and $\tan\delta$ by measuring compound structures consisting of two layers compared to the values obtained from measuring the single layers are 1.34% and 71.44%, respectively. The errors by measuring compound structures consisting of three layers are 1.73% and 145.44%, respectively.

In order to verify the convergence of the new method, the simulations are performed several times. In Table IV, the standard deviations $\sigma_{\varepsilon'}$ and $\sigma_{\tan\delta}$ of the material parameters ε' and $\tan\delta$, respectively, are given for ten program runs. In each run, different start values have been used for the random number generator. High standard deviations are only found for the imaginary permittivities $\tan\delta$ of Al_2O_3 and Teflon. In contrast, the real permittivities ε' of all three materials as well as the imaginary permittivity $\tan\delta$ of Macor can be determined with a very high accuracy and reproducibility (see Table IV).

V. FEATURES AND LIMITATIONS OF THE PROCEDURE

The presented method to extract the material parameters of compound multilayered structures needs scalar reflection and/or transmission measurement data over the frequency or over the angle of incidence. The thicknesses of the single layers have to be at least in the range of the wavelength. Characteristic minima caused by negative interference have to appear inside the measured frequency or angular range because therewith the material parameters can be determined. Therefore, dispersive materials have to be measured at one frequency over the angle and perhaps for different polarizations. In principle, frequency-dependent parameters (e.g., $\underline{\varepsilon}_n$ as a function of f) could also be introduced in the GA, but this would increase the number of unknowns and therewith reduce the accuracy. Instead of using frequency-dependent parameters, the total frequency range can be divided

TABLE IV
STANDARD DEVIATIONS OF THE MATERIAL PARAMETERS GIVEN IN TABLE III CALCULATED FROM TEN PROGRAM RUNS

measured structures	Al_2O_3		Macor		Teflon	
	$\sigma_{\varepsilon'}$	$\sigma_{\tan\delta}$	$\sigma_{\varepsilon'}$	$\sigma_{\tan\delta}$	$\sigma_{\varepsilon'}$	$\sigma_{\tan\delta}$
single layers	0	0	0	0	0	0
Al_2O_3-Macor	0	$0.02 \cdot 10^{-3}$	0	0	-	-
Al_2O_3-Teflon	0	$0.18 \cdot 10^{-3}$	-	-	0	$0.12 \cdot 10^{-3}$
Macor-Teflon	-	-	0	0	0	$0.01 \cdot 10^{-3}$
Al_2O_3-Macor-Teflon	0	$1.31 \cdot 10^{-3}$	0	0.002	0	$0.51 \cdot 10^{-3}$
Al_2O_3-Teflon-Macor	0.01	$4.78 \cdot 10^{-3}$	0.02	0.006	0.18	$6.86 \cdot 10^{-3}$
Macor-Al_2O_3-Teflon	0.01	$4.18 \cdot 10^{-3}$	0.01	0.008	0	$0.61 \cdot 10^{-3}$

in intervals in which the parameters can be assumed to be constant. This method was successfully applied on measurements that have been performed with three layered windscreens [15], [16]. The sensitivity level of the measurement system limits the accuracy of the detected small imaginary parts of the permittivities as they define the depths of the minima.

VI. CONCLUSIONS

In this paper, a new method has been presented that determines the material parameters of each single layer of a compound multilayered structure. The shown GA uses measurements of the compound structure to determine the parameters of the single layers. The measurements are either performed versus frequency or versus different angles of incidence. The GA shows good stability and produces accurate results. This technique is well suited for bonding materials where the single layers cannot be measured separately. The algorithm has also been applied successfully on windscreens consisting of three layers [15], [16].

If single layers are measured and their material parameters are determined by the new method, a very high accuracy can be reached. The accuracy of the determination of the material parameters by measuring one single layer is only limited by the accuracy of the measurement setup, but not by the algorithm. As more layers are measured together, the error increases. The low accuracy in the determination of the relatively small imaginary parts of Al_2O_3 and Teflon is caused by the limited sensitivity level of the measurement system. The larger imaginary part of Macor could be more accurately determined.

ACKNOWLEDGMENT

The authors would very much like to thank Dr. O. Braz, Institut für Hochleistungsimpuls- und Mikrowellentechnik (IHM), Forschungszentrum Karlsruhe, Germany, for providing his angular-dependent reflection measurements of Quartz glass and Si_3N_4. The authors also would very much like to thank A. Arnold, IHM, Forschungszentrum Karlsruhe, for the excellent assistance with the measurements of Al_2O_3, Macor, and Teflon.

REFERENCES

[1] R. Schwab, R. Spörl, J. Burbach, and R. Heidinger, "MM-wave characterization of low loss dielectric materials using open resonators," in *ITG-Fachbericht 150: Displays and Vacuum Electronics*. Berlin, Germany: VDE–Verlag, 1998, pp. 363–368.

[2] R. Heidinger and G. Link, "The temperature dependence of the permittivity in high-power and broadband mm-wave window materials," in *Proc. 6th Russian–German ECRH Gyrotrons Meeting*, Moscow, Russia, 1994, pp. 271–292.

[3] M. N. Afsar and K. J. Button, "Millimeter-wave dielectric properties of materials," in *Infrared and Millimeter Waves*. New York: Academic, 1984, vol. 12, pp. 1–42.

[4] F. Sobel, F. L. Wentworth, and J. C. Wiltse, "Quasioptical surface waveguide and other components for the 100 to 300 GHz region," *IRE Trans. Microwave Theory Tech.*, vol. MTT-9, pp. 512–518, 1961.

[5] C. A. Balanis, *Advanced Engineering Electromagnetics*. New York: Wiley, 1989, ch. 5.

[6] I. Rechenberg, *Evolutionsstrategie* (in German). Stuttgart, Germany: Frommann-Holzboog, 1973, ch. B.

[7] D. E. Goldberg, *Genetic Algorithms in Search, Optimization and Machine Learning*. Reading, MA: Addison-Wesley, 1989, ch. 1–3.

[8] R. L. Haupt, "An introduction to genetic algorithms for electromagnetics," *IEEE Antennas Propagat. Mag.*, vol. 37, pp. 7–15, Apr. 1995.

[9] J. M. Johnson and Y. Rahmat-Samii, "Genetic algorithms in engineering electromagnetics," *IEEE Antennas Propagat. Mag.*, vol. 39, pp. 7–25, Apr. 1997.

[10] A. Hippel, *Dielectric Materials and Applications*. Norwood, MA: Artech House, 1995, ch. V.

[11] T. Geist, G. Hochschild, and W. Wiesbeck, "Scalar millimeter-wave network analysis with high dynamic range," in *Proc. 18th Eur. Microwave Conf.*, Stockholm, Sweden, 1988, pp. 339–343.

[12] H.-U. Nickel, "Hochfrequenztechnische Aspekte zur Entwicklung Rückwirkungsarmer Ausgangsfenster für Millimeterwellengyrotrons Hoher Leistung," Ph.D. dissertation (in German), Forschungszentrum Karlsruhe, Karlsruhe, Germany, 1995.

[13] O. Braz, G. Dammertz, M. Kuntze, and M. Thumm, "D-band frequency step-tuning of a 1 MW gyrotron using a Brewster output window," *Int. J. Infrared Millim. Waves*, vol. 18, pp. 1465–1477, 1997.

[14] O. Braz, "Meßtechnische Untersuchungen zur Hochfrequenzauskopplung an Millimaterwellengyrotrons Hoher Leistung," Ph.D. dissertation (in German), Forschungszentrum Karlsruhe, Karlsruhe, Germany, 1998.

[15] T. Zwick, K. Schmitt, and W. Wiesbeck, "Radio communication through car windows," *Automobiltechnische Zeitschrift*, no. 4, pp. 220–226, 1997.

[16] R. Schertlen, T. Zwick, and W. Wiesbeck, "Characterization of car windows for transmission of millimeter-waves," in *Eur. Microwave Conf.*, Paris, France, Oct. 2000, pp. 115–118.

Thomas Zwick (S'94–A'99–M'00) was born in Ludwigshafen/Rhein, Germany, in 1970. He received the Dipl.-Ing. (M.S.E.E.) and Dr.-Ing. (Ph.D.E.E.) degrees from the Universität Karlsruhe (TH), Karlsruhe, Germany, in 1994 and 1999, respectively.

From 1994 to 2001, he was Research Assistant with the Institut für Höchstfrequenztechnik und Elektronik (IHE), Universität Karlsruhe (TH). Since February 2001, he has been with the IBM T. J. Watson Research Center, Yorktown Heights, NY. His research interests include electromagnetic-wave propagation, channel measurement techniques, material measurements, stochastic channel modeling, and wireless communication system design. He has participated as an expert in the European COST231 Evolution of Land Mobile Radio (Including Personal) Communications and COST259 Wireless Flexible Personalized Communications. For the Carl Cranz Series for Scientific Education, he served as a Lecturer for *Wave Propagation*.

Jens Haala (S'96–M'01) was born in Heilbronn, Germany, in 1970. He received the Dipl.-Ing. (M.S.E.E.) and Dr.-Ing. (Ph.D.E.E.) degrees from the Universität Karlsruhe (TH), Karlsruhe, Germany, in 1996 and 2000, respectively.

From 1996 to 2001, he was a Research Assistant with the Institut für Höchstfrequenztechnik und Elektronik (IHE), Universität Karlsruhe (TH). Since January 2001, he has been with Marconi Communications Software Systems, Backnang, Germany. His research interests include electromagnetic compatibility, microwave heating, and material measurements, as well as numerical modeling of electromagnetic-wave propagation and microwave heating.

Werner Wiesbeck (SM'87–F'94) received the Dipl.-Ing. (M.S.E.E.) and Dr.-Ing. (Ph.D.E.E.) degrees from the Technical University of Munich, Munich, Germany, in 1969 and 1972, respectively.

From 1972 to 1983, he was with AEG-Telefunken in various positions, including that of Head of Research and Development, Microwave Division, Flensburg, Germany, and Marketing Director Receiver and Direction Finder Division, Ulm, Germany. During this period, he had product responsibility for millimeter-wave radars, receivers, direction finders, and electronic-warfare systems. Since 1983, he has been the Director of the Institut für Höchstfrequenztechnik und Elektronik (IHE), Universität Karlsruhe (TH), Karlsruhe, Germany. His research interests include radar, remote sensing, wave propagation, and antennas. In 1989 and 1994, respectively, he spent a six-month sabbatical at the Jet Propulsion Laboratory, Pasadena, CA. For the Carl Cranz Series for Scientific Education, he serves as a permanent Lecturer for *Radar System Engineering* and *Wave Propagation*.

Dr. Wiesbeck was a member of the IEEE Geoscience and Remoting Sensing Society (IEEE GRS-S) Administrative Committee (AdCom) (1992–2000), chairman of the IEEE GRS-S Awards Committee (1994–1998), executive vice president of the IEEE GRS-S (1998–1999), president of the IEEE GRS-S (2000–2001), associate editor of the IEEE TRANSACTIONS ON ANTENNAS AND PROPAGATION (1996–1999), and past treasurer of the IEEE German Section. He is a member of an Advisory Committee of the European Union (EU)–Joint Research Centre (Ispra/Italy). He is an advisor to the German Research Council (DFG), the Federal German Ministry for Research (BMBF), and industry in Germany. He was general chairman of the 1988 Heinrich Hertz Centennial Symposium, the 1993 Conference on Microwaves and Optics (MIOP'93), and scientific committee member of numerous conferences.